

A HYBRID BEM/SINGULAR SUPERPOSITION ALGORITHM TO SOLVE THE INVERSE GEOMETRIC PROBLEM APPLIED TO SUBSURFACE CAVITY DETECTION

Alain J. Kassab

*Mechanical, Materials, and
Aerospace Engineering
University of Central Florida
Orlando, Florida, 32816, USA
kassab@mail.ucf.edu*

Eduardo A. Divo

*Engineering Technology
Departement
University of Central Florida
Orlando, Florida, 32816, USA
edivo@mail.ucf.edu*

Andreas Hadjinicolaou

*Siemens-Westinghouse
Power Corporation
4400 Alafaya Trail
Orlando, Florida, 32826, USA
andreas.hadjinicolaou@siemens.com*

ABSTRACT

A method is presented for the efficient solution of the inverse geometric problem applied to detection of subsurface cavities and flaws using thermographic techniques. A hybrid method, consisting of the superposition of clusters of sources/sinks coupled to a boundary element solution, is developed for the solution of the forward problem. The numerical scheme avoids re-meshing of the interior geometry as it evolves in the process of solving the inverse problem iteratively to detect the subsurface flaw or cavity. The hybrid approach markedly reduces the computational burden involved in re-meshing and presents a promising technique for 3D applications.

INTRODUCTION

This paper concerns the solution of the inverse geometric problem which finds application in the nondestructive evaluation of subsurface flaws and cavities. The governing equation, thermophysical properties, boundary conditions, and that portion of the geometry that is exposed are all known, while, the portion of the geometry that is hidden from view is to be characterized with the help of an over-specified (Cauchy) condition at the exposed surface, see Fig. 1. Specifically, the surface temperature and heat flux is given at the exposed surface, and the geometry of the cavity(ies) that generated the measured temperature footprint is to be determined. The boundary condition at the cavity side can be specified as either homogeneous or non-homogeneous first, second, or third kind of boundary condition.

Solution of the inverse geometric problem can be undertaken by analyzing either the transient or steady state thermal response of a system subjected to a thermal load. This leads to two classes of techniques: transient based thermal wave imaging methods [1-2] and steady state based methods [3-5]. We are concerned with the latter for which Ramm [6] demonstrates mathematically that a unique solution exists for media with constant thermal conductivity.

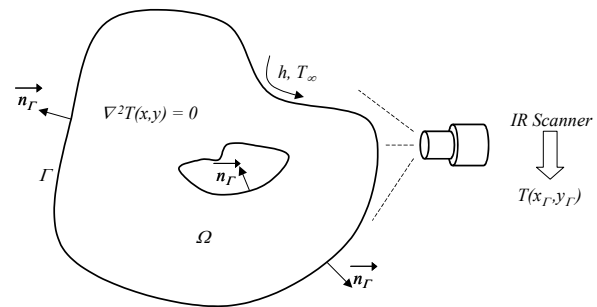


Figure 1. The inverse geometric heat conduction problem identifying a subsurface cavity using surface temperatures measured by thermographic methods illustrated here as using an infrared scanner.

The inverse geometric problem which has been solved by a variety of numerical methods [7-14], or its closely shape optimization [15-18], is arguably the most computationally intensive of inverse heat transfer problem. This is due to its inherent nature requiring a complete re-generation of the mesh as the geometry evolves regardless of whether a numerical or analytical approach is taken to solve the associated direct problem. Moreover, the continuous evolution of the geometry itself poses certain difficulties in arriving at analytical or numerical sensitivity coefficients [19-21] for gradient-based optimization approaches and in the updates of the subsurface geometry(ies) and associated mesh(es), particularly in 3D, whether using domain meshing methods such as finite element or finite volume methods or boundary meshing method such as boundary elements [22-24]. There arises the need for an efficient technique that avoids the implicit requirement of performing completely new solutions as the geometry is sought, particularly in 3D applications.

We adopt a hybrid singular superposition/BEM method developed by the authors [25] for the efficient solution of the inverse geometric problem of detection of subsurface cavities and flaws using thermographic

techniques and apply this to a three-dimensional inverse geometric problem. Here, a superposition of clusters of sources/sinks with a BEM solution of the forward problem offers a numerical scheme that does not require re-meshing of the interior geometry as inverse problem is solved iteratively to detect the flaw or cavity. The location of the cluster or clusters and strengths of the sources/sinks within the cluster is first determined to satisfy Cauchy conditions at the exposed surface. The clusters must locate themselves within the cavity(ies) if such are present or outside the problem domain, if there are no cavities enclosed in the domain, in order to satisfy the governing Laplace equation. Subsequent to the location of the cluster(s) and strength of the associated strengths of the sources/sinks within the cluster(s), a search is initiated to located the internal geometry corresponding to the enclosed cavity(ies) that satisfies the boundary condition at the cavity side. The latter is taken as adiabatic in this study. Although prescribing an adiabatic condition is not necessary for the algorithm developed herein, this is rather an example of a practical imposition of a boundary condition at the cavity side, and in this case offers is good model of an air pocket type inclusion. Both the location of the cluster(s) and associated strengths of the sources/sinks and the search for the cavity geometry is accomplished using a genetic algorithm (GA). The approach offers tremendous advantage in reducing the computational burden involved in re-meshing and presents a very promising technique for 3D applications. Moreover, the method can be readily extended to the closely-related design problem of shape optimization of thermal systems and may be extended to other field problems of NDE using surface displacements in an elasticity-based approach to solving the inverse geometric problem [26,27].

FORMULATION OF THE INVERSE SOLUTION ALGORITHM

In steady-state inverse geometric problem under consideration, the governing equation is the Laplace equation, the heat flux and temperature at the exposed surface of the body are both known and thus specified, and the boundary condition at the cavity side is specified as adiabatic. The geometry of the cavity is, however, unknown and to be determined as the goal of the solution of the inverse problem. There are three components to the solution algorithm:

- (1) the forward problem solver: a hybrid BEM/singularity method.
- (2) inverse problem solver: GA to locate and fix singularity cluster strengths to match Cauchy conditions imposed at exposed boundary.

- (3) cavity shape detection: GA to locate cavity walls.

The Forward Problem Solver

The problem of steady heat conduction in homogeneous media is governed by the Laplace equation in analogy with the behavior of the velocity potential and the stream function in ideal fluid flow problems. The superposition of singular potentials in an incoming flow is known to generate shapes characterized by curves of constant stream function value that are impervious to the flow. In a heat conduction problem, the existence of a cavity can be characterized by an internal adiabatic contour. Such contour can be artificially construed by counterbalancing the heat flow generated by external boundary conditions with the heat flow generated by singular perturbations such as sources and sinks of different strengths. These singularities must be located within the cavity(ies) and thus outside the domain problem to satisfy the Laplace equation, see Fig. 2. The underlying concept of the method is thus borrowed from potential flow theory, where, for example, the superposition of a doublet of appropriately fixed strength to counteract an incoming uniform flow generates an impervious cylindrical surface or the superposition of an appropriately placed and calibrated source and sink counteract a uniform incoming flow to generate a Rankine oval with a surface impervious to the incoming flow.

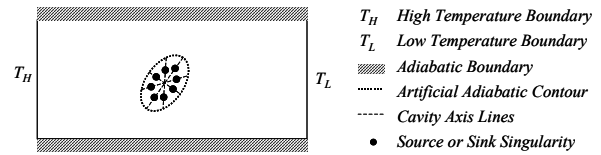


Figure 2. Singularity superposition configuration.

The mathematical formulation that follows this idea consists of the Poisson equation for the temperature $T(x)$ where the generation term is the summation of singular field perturbations characterized by K -localized Dirac delta functions as:

$$\kappa \nabla^2 T(x) + \sum_{k=1}^K \left(-\hat{Q}_k \right) \delta(x, x_k) = 0 \quad (1)$$

where κ is the thermal conductivity, \hat{Q}_k represents the strength of the perturbation positive for a source and negative for sink, and x_k represents the perturbation locations which in the final solution have to be located within the internal cavity, or external to the body, otherwise the Laplace equation would be violated.

The above equation is solved by the Boundary Element Method (BEM), a numerical technique that lends itself ideally to the problem due to its boundary-only discretization feature and its ability to relate the field variable values anywhere in the domain to the information along the boundary. These characteristics of the BEM will make it possible to isolate the effects of the added singular perturbations and compute the field variable values only where necessary. A standard BEM formulation starts with the introduction of a free-space fundamental solution $G(x, \xi_i)$ and a transformation of the governing equation into an integral equation over the domain Ω . Green's second identity is applied to the domain integral to transform it into contour integrals over the boundary Γ as:

$$C(\xi_i)T(\xi_i) - \oint_{\Gamma} T(x)H(x, \xi_i)d\Gamma = \quad (2)$$

$$+ \oint_{\Gamma} q(x)G(x, \xi_i)d\Gamma = \sum_{k=1}^K \hat{Q}_k G(x_k, \xi_i)$$

where $H(x, \xi_i) = -\kappa \frac{G(x, \xi_i)}{\partial n}$, $q(x) = -\kappa \frac{\partial T(x)}{\partial n}$, and $C(\xi_i)$ depends on the geometry and location of the source point ξ_i . Following the discretization of the boundary Γ with N -nodal locations and the collocation of the source point ξ_i at these N -locations, the above boundary integral equation reduces to the standard form:

$$\sum_{j=1}^N G_{ij}q_j = \sum_{j=1}^N H_{ij}T_j + \sum_{k=1}^K G_{ik}\hat{Q}_k \quad (3)$$

We used quadratic discontinuous elements in all our computations [24]. Provided that a well-posed problem is available with a properly defined geometry and set of boundary conditions, the above equation is collocated to provide a set of linear equations of the form $A_{ij}x_j = b_i + S_i$ with $i = 1 \dots N$ and where S_i contains the effects of the added singularities \hat{Q}_k . The solution to this system provides the full distribution of temperatures and fluxes around the boundary that can later be used in the same formulation to calculate these variables anywhere in the domain Ω . It is note that only an exterior discretization is required in this forward problem formulation.

The Inverse Problem Solver

In the inverse case where the location, size, and shape of the cavity are unknown, the strengths of the added singularities may be adjusted to counteract the heat flow generated by the boundary conditions imposed at the exterior boundary and to consequently produce the artificial adiabatic contour enclosing them.

This can be accomplished by the minimization of a functional that reduces the standard deviation of the successively BEM-computed temperatures T_i at the $i = 1, 2 \dots N_m$ measuring points with respect to the N_m measured temperatures \hat{T}_i at the exposed boundaries, and formally,

$$S(\hat{Q}_k, z) = \sqrt{\frac{1}{N_m} \sum_{i=1}^{N_m} (T_i - \hat{T}_i)^2} \quad (4)$$

This objective function depends on the singularity strengths, \hat{Q}_k , and a number of other parameters z to be shortly specified. It may be regularized by adding an explicit damping term other techniques, such as proper selection of an iterative stopping criterion, when using gradient-based techniques. However, when using the non-gradient-based genetic algorithm (GA) [28] adopted in this study, the smoothing property inherent in the algorithm permits solution without explicit regularization.

In solving inverse problems it is important to keep the sought-after parameters to a minimum. To this end, in 2-D, each cavity is characterized by a cluster of $K = 8$ singularities located on the discrete edges of a rotated ellipse defined by thirteen parameters:

- (a) strengths, \hat{Q}_k , of 8 equally distributed singularities around the edge of an ellipse,
- (b) x and y locations of the centroid of the ellipse,
- (c) r_x - and r_y -lengths of axes of the ellipse,
- (d) angle α of rotation with respect to the x -axis.

The explicit dependency of the objective function in Eqn. (4) on these thirteen parameters will provide enough degrees of freedom to locate a basic but generally-shaped cavity.

In 3-D, each cluster is comprised of a sequence of ever increasing number of parameters in a 3 level search. It is noticed from 2-D computations that the location of the center of the cluster is readily found within the first few GA generations and subsequently much effort is expended in adjusting strengths to satisfy imposed external boundary conditions. Thus, initially, the cluster is composed of six singularities with one at each pole of an ellipsoid and four equally distributed on a ring at the ellipsoid equator, thus unknowns appearing in the GA are the six strengths of the singularities, x -, y -, and z -locations of the ellipsoid centroid, its major and minor axes, and two angles defining its inclination or a total of 13 unknowns. The GA searches all the allowable space within the external domain enclosure. Once the centroid is located, the next level of search is carried out, by increasing the

number of singularities to 14 singularities (2 located at the poles of the ellipsoid and 12 located on two rings equally spaced from the poles along the long axis of symmetry each ring bearing 6 singularities). However, in this search of the GA, the geometric search space is reduced diminishing the roaming range of the centroid to locations close to that found by the first model. Next, a third level finer search is carried out with 26 singularities (2 located at the poles of the ellipsoid and 24 located on three rings equally spaced from the poles along the long axis of symmetry each ring bearing 8 singularities). In this final search of the GA, the geometric search space is diminished even further than in the previous level.

As the inverse problem is now well-defined, a means of minimization of the functional must be sought to be able to provide a global approximation that disregards the multiple local minima that will appear as a result of the inherent non-linearity of this problem. This feature along with many more can be found in the Genetic Algorithms (GA) lending themselves perfectly for such application. GA are robust adaptive search techniques that mimic the idea of Darwinian evolution using rules of natural selection to investigate highly complex multidimensional problems. As a non-gradient-based optimization technique the use of GA is advantageous for this until a best-fit is found that application. The parameters that characterize the existence of the cavity may be progressively adjusted by the operators of the GA maximizes a fitness function. This fitness function can be easily and directly defined as the inverse of the least-square functional $S(\hat{Q}_k, z)$ as:

$$Z(\hat{Q}_k, z) = 1/S(\hat{Q}_k, z) \quad (5)$$

The combination of these techniques in the shape optimization problem minimizes the need for computationally intensive algorithms as no new discretizations are required for the solution of different direct problems along the optimization process. These solutions are achieved by simply changing the right-hand side vector of a linear system of equation whose coefficient matrix is calculated and factorized only once. These features offer a tremendous computational savings in 3-D cavity detection. Once the strengths of the singularities and their location is determined by locating their carrier ellipse, there remains the task of finding the adiabatic line corresponding to the sought after cavity. Here, an optimization problem is solved.

Cavity Shape Location

Locating the cavity is now the problem of searching the continuous domain enclosed by the

exterior boundary for the location of the adiabatic. Consequently, the integral equation, Eqn. (2), is differentiated with respect to the x_i and y_i discrete locations around the edge of a rotated ellipse in 2-D that surrounds the singularity cluster, see Fig. 3, or a rotated ellipsoid in 3-D, in order to provide the heat flux $q(x_i, y_i) = -\kappa \partial T(x_i, y_i)/\partial n$. Thus, a second optimization problem is solved to adjust the five parameters of a rotated ellipse (x, y, r_x, r_y, α) that surrounds the cluster until heat fluxes are minimized. This is again accomplished using a genetic algorithm with fitness function:

$$Z(x, y, r_x, r_y, \alpha) = \left(\sqrt{\frac{1}{N_q} \sum_{j=1}^{N_q} (q_j)^2} \right)^{-1} \quad (6)$$

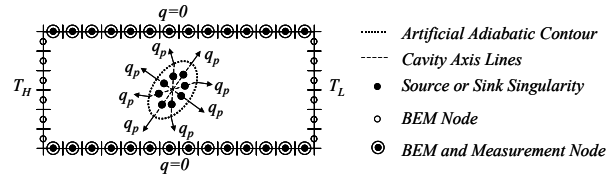


Figure 3. BEM discretization and inverse problem configuration.

The Genetic Algorithm

The GA optimization process begins by setting a random set of possible solutions, called the population, with a fixed initial size or number of individuals. Each individual is defined by optimization variables and is represented as a bit string or a chromosome, see Fig. 4. An objective function, Z_{GA} , is evaluated for every individual in the current population defining the fitness or their probability of survival. At each iteration of the GA, the processes of selection, cross-over, and mutation operators are used to update the population of designs. A selection operator is first applied to the population in order to determine and select the individuals that are going to pass information in a

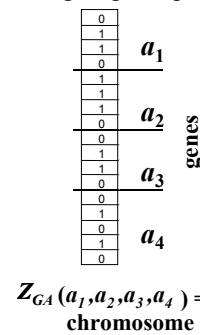


Figure 4. Example of an individual in the population characterized by four parameters (genes) encoded in a chromosome yielding the individual's fitness value F_1 .

mating process with the rest of the individuals in the population. This mating process is called the crossover operator, and it allows the genetic information contained in the best individuals to be combined to form offsprings. Additionally, a mutation operator randomly affects the information obtained by the mating of individuals. This is a crucial step for continuous improvement.

In the GA we used to generate results presented in the example section, the following parameters are chosen: population size of 50 individuals/generation, with a strings of 8 bits for the position, strength, and radii, and five bits for each angle. The mating process produces one children per mating using uniform crossover which produces a higher level of diversity than single point cross-over, a 4% probability of jump mutation, 20% probability of creep mutation, and 50% probability of crossover. The population is not allowed to grow (static population) and elitistic generation (the best parent survives to the next generation). The population is completely eliminated after 50 generations if there is no further improvement, keeping the best member of the population (restart). We use no micro-generation, the practice of periodically decreasing of the population size with a sharp increase in mutation in an effort to create further diversity in large problems. This combination of parameters and procedures has been proven to yield efficient and accurate optimization results for different studies carried out in this paper. This completes the theoretical developments in this paper, attention is now given to numerical examples in 2-D and 3-D that are used to illustrate the algorithm developed above for the solution of the inverse geometric problem.

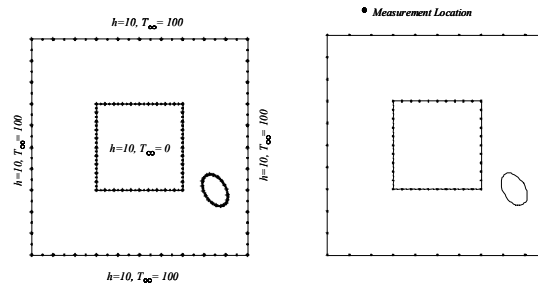
NUMERICAL EXAMPLES

In the numerical examples considered in this section, a forward problem is solved using the BEM to first to generate boundary conditions at the external surface. Discontinuous boundary elements are used in all cases and adaptive quadratures are implemented in the 2D and 3D BEM codes. These are in turn used to simulate inputs to the inverse problem. Random error is then added to surface temperatures to simulate measurement error/uncertainty in the range of expected accuracy in measured temperatures.

Numerical studies [25] established the trend that clusters relatively quickly locate the center of the cavity in the first iterations and then spend the rest of the iterations adjusting the singularity strengths. This trend can readily be exploited in 3D applications where an educated sequentially more refined search is performed: a coarse cluster is first used to locate the

center of the cavity, followed by increasingly refined clusters searching in a reduced spatial domain close to the estimated cavity center. When a non-existent hole is sought by the algorithm, within a generation the cluster(s) move outside the simply or multiply-connected domain and remain there in all subsequent iterations, otherwise the Laplace equation would be violated. Furthermore, the size of the cluster(s) reduce to a very small surface, a hint that can be used in future simulations to eliminate clusters that may not contribute to the solution of the problem.

This is illustrated in the 2D example problem where an attempt is made to locate an elliptic hole centered at $(x, y) = (0.85, 0.3)$ with minor and major axes $(r_x, r_y) = (0.05, 0.08)$ and tilted at an angle $\alpha = \pi/6$ and located within the doubly connected plate. The elliptic hole is discretized using 20 quadratic boundary and the plate is discretized using 40 quadratic discontinuous boundary elements on each boundary, see Fig. 5(a) for the geometry and boundary conditions used in the forward problem, and Fig. 5(b) for the location of the measurements used in the solution of the associated inverse geometric problem. The detection of the cavity is carried out using temperature inputs from the direct problem which are laden with ± 0.25 degrees maximum random error.



(a) BEM mesh and boundary conditions. (b) sensor locations for temperature measurements.

Figure 5. Locating a tilted elliptical cavity enclosed in a doubly-connected square plate.

First, we send two clusters to search for the single cavity and the evolution of the search is provided in Fig. 6(a)-(f). Notice that one cluster locates itself inside the cavity, while the other exits the doubly-connected domain and shrinks to a very small area. As such, that cluster is eliminated, and the search is continued with the single surviving cluster. Finally, the cavity is successfully located, see Fig. 6(f). The objective function evolution for the cluster identification and hole location are displayed in Fig. 7(a)-(c). This example illustrates how to seek a cavity and answers the question as to how many clusters to launch.

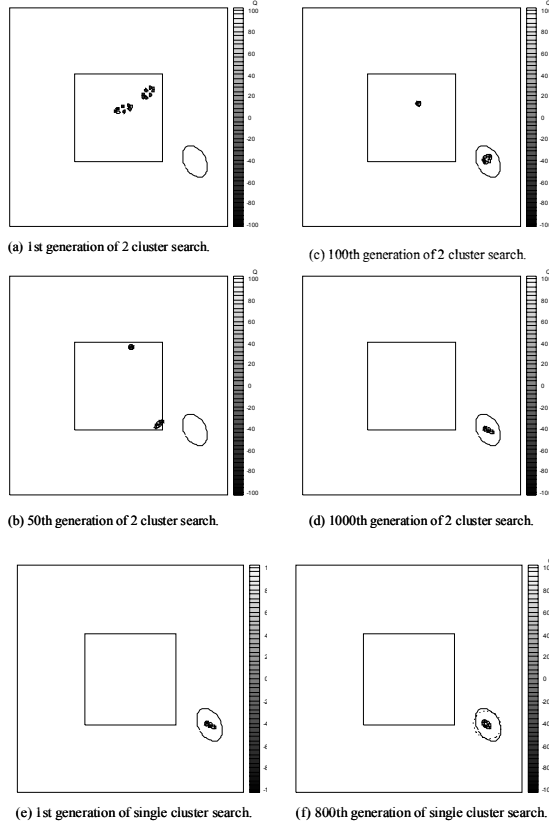
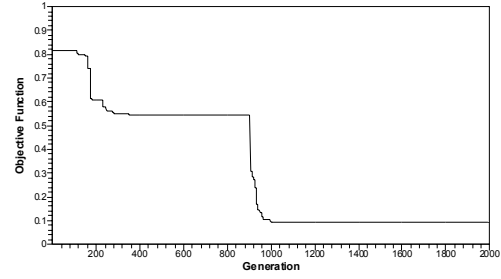


Figure 6. Cluster identification with ± 0.25 simulated input random error in temperatures.

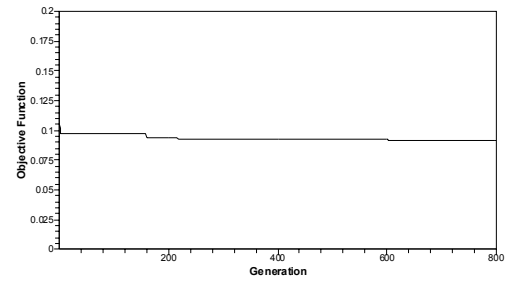
The second example is a challenging 3D application where we seek a cavity located within a $(1 \times 1 \times 1)$ parallelepiped with a rectangular plenum in the z -direction of x - y size (0.4×0.4) . A spherical cavity whose center is located at $(0.4, 0.4, 0.2)$ and with radius (0.075) is to be located, see Fig. 8. Ninety six discontinuous bilinear boundary elements are used to discretize the problem and convective conditions imposed on exposed surfaces: $T_\infty = 100$, $h = 5$ on outside wall; $T_\infty = 100$, $h = 20$ on bottom wall $z = -0.5$; $T_\infty = 0$, $h = 30$ on inside wall; $T_\infty = 0$, $h = 20$ on top wall at $z = 0.5$. There are 728 measuring points located at each element midpoint. Simulated surface temperatures were ladened with random errors with a maximum of ± 0.25 degrees. Cluster identification was performed using three levels of increasingly refined search space and increasing number of singularities in the cluster:

- (a) Search in full space: x from -0.5 to 0.5 ; y from -0.5 to 0.5 ; z from -0.5 to 0.5 ; 6 singularities.
- (b) Search in limited space: x from 0.2 to 0.5 ; y from 0.2 to 0.5 ; z from 0 to 0.5 ; 14 singularities.
- (c) Search in narrow space: x from 0.35 to 0.45 ;

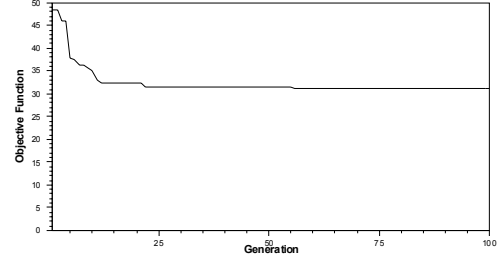
y from 0.35 to 0.45 ; z from 0.15 to 0.25 ; 26 singularities.



(a) objective function evolution for two-cluster identification ($F = 0.093$)



(b) objective function evolution for one-cluster identification ($F = 0.09$)



(c) objective function evolution for hole identification ($F = 31.23$).

Figure 7. Objective function evolution for the detection of an elliptical cavity within a doubly-connected plate.

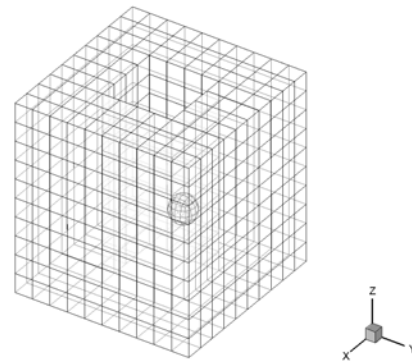


Figure 8. BEM mesh and cavity for the 3D example.

Results of the cavity detection are displayed in Figs. 9(a) and 9(b) for the 1st level of search, while the coarse 6 singularity cluster final location after 2000 GA generations is shown in a close-up in Fig. 10(a). It is noted that the cluster is located within the actual cavity. Now that cluster location has settled, the next level of refinement in the search is undertaken by increasing the number of singularities from 6 to 14 while restricting the geometric search space to a region close to the converged location of the coarse 6 singularity cluster. Finally, a refined search is carried out by increasing the cluster to 26 singularities with an even more restrictive geometric search space. Results are displayed in Fig. 10(a)-(c) and the final detected cavity is compared to the exact cavity in Fig. 10(d). It is clear that the cavity is successfully detected in terms of its location and size.

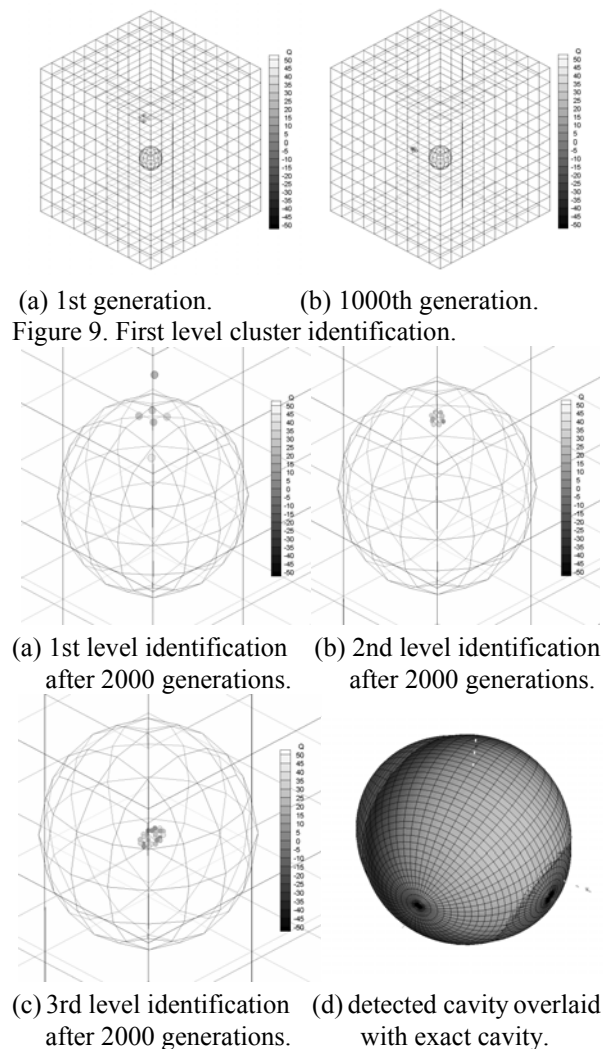


Figure 10. Zoom-in of converged first, second and third levels of refinement in cluster identification and comparison of exact and detected cavity.

CONCLUSIONS

We present a hybrid BEM/singularity superposition method for the detection of subsurface cavities and flaws using thermographic techniques. A genetic algorithm is used to solve the inverse problem locating of the cluster(s) of singularities and fixing their strengths and subsequently identifying the cavity geometry. An adiabatic condition is taken at the cavity side, as this is the most feasible condition to assume in an inverse detection problem. The method does not require re-meshing of the interior geometry as the inverse problem is solved iteratively. The approach thus significantly reduces algorithmic complexity and computational burden. Examples demonstrate the ability of the method to successfully locate location and size of a single and multiple cavities. The technique is readily applicable to the closely related problem of shape optimization, where the condition at the cavity side may be arbitrarily specified as a design target. The authors are pursuing extensions of the method to an elasticity approach to solving the inverse geometric problem using surface displacements information.

REFERENCES

1. Maldague, X., *Non Destructive Evaluation of Materials by Infrared Thermography*, Springer-Verlag, New York, 1992.
2. Favro, L., Crowther, J.D., Kuo, P.K. and Thomas, R.L., Inversion of Pulsed Thermal Wave Images for Defect Sizing and Shape Recovery, *SPIE*, Vol. 1682, *Thermosense XIV*, pp. 178-181, 1992.
3. Hsieh, C. K. and Su, K.C., A Methodology of Predicting Cavity Geometry Based on the Scanned Surface Temperature Data-Prescribed Surface Temperature at the Cavity Side, *Journal of Heat Transfer*, Vol. 102, pp. 324-329, 1980.
4. Hsieh, C.K. and Su, K.C., A Methodology of Predicting Cavity Geometry Based on the Scanned Surface Temperature Data-Prescribed Heat Flux at the Cavity Side, *Journal of Heat Transfer*, Vol. 103, pp. 42-46, 1981.
5. Hsieh, C.K., Wang, X.A., and Yang, S.L., Infrared Scanning Thermography for a Quantitative Detection of Cavities in a Plane Slab and Rectangular Prism, *Journal of Nondestructive Evaluation*, Vol. 3, pp. 99-109, 1982.
6. Ramm, A.G., A Geometrical Inverse Problem, *Inverse Problems*, Vol. 2, L19-L21, 1986.
7. Huang, C.H. and Chao, B.-H., Inverse Geometry Problem in Identifying Irregular Boundary Configurations, *Int. J. Heat and Mass Transfer*, Vol. 40, No. 9, pp. 2045-2053, 1997.

8. Kassab, A.J., Hsieh, C.K., and Pollard, J., Solution of the Inverse Geometric Problem for the Detection of Subsurface Cavities by the IR CAT Method, in L.C. Wrobel and D.B. Ingham, (eds.), *Boundary Integral Formulations in Inverse Analysis*, Chapter 2, Computational Mechanics, Boston, 1997.
9. Dulikravich, G.S. and Martin, J.M., Geometrical Inverse Analysis Problems in Three-Dimensional Non-Linear Steady Heat Conduction, *Engineering Analysis with Boundary Elements*, Vol. 15, pp. 161-169, 1995.
10. Kassab, A.J. and Pollard, J., Automated Cubic Spline Anchored Grid Pattern Algorithm for the High Resolution Detection of Subsurface Cavities by the IR-CAT Method, *Numerical Heat Transfer, Part B: Fundamentals*, Vol. 26, No. 1, pp. 63-78, 1994.
11. Kassab, A.J. and Pollard, J., Automated Algorithm for the Nondestructive Detection of Subsurface Cavities by the IR-CAT Method, *J. Nondestructive Evaluation*, Vol. 12, No. 3, pp. 175-187, 1993.
12. Das, S. and Mitra, A., An Algorithm for the Solution of Inverse Laplace Problems and its Application in Flaw Identification in Materials, *J. Computational Physics*, Vol. 99, pp. 99-105, 1992.
13. Kassab, A.J. and Hsieh, C.K., Application of Infrared Scanners and Inverse Heat Conduction Problems to Infrared Computerized Axial Tomography, *Review of Scientific Instruments*, Vol. 58, No. 1, pp. 89-95, 1987.
14. Hsieh, C.K. and Kassab, A.J., A General Method for the Solution of Inverse Heat Conduction Problems with Partially Unknown System Geometries, *Int. Journal of Heat and Mass Transfer*, Vol. 29, No. 1, pp. 47-58, 1985.
15. Burczynski, T., Beluch, W., Dlugosz, A., Kus, W., Nowakowski, M., and Orantek, P., Evolutionary Computation in Optimization and Identification, *Computer Assisted Mechanics and Engineering Sciences*, Vol. 9, No. 1, pp. 3-20, 2002.
16. Nordlund, R.S. and Kassab, A.J., A Conjugate BEM Optimization Algorithm for the Design of Turbine Vane Cooling Channels, *BETECH96: Proc. of 12th Int. Boundary Element Tech. Conf.*, Hawaii, Ertekin, E.K., Tanaka, M., Shaw, R.P. and Brebbia, C.A. (eds.), pp. 237-246, Computational Mechanics, Southampton and Boston, 1996.
17. Cheng, C.H. and Wu, C.Y., An Approach Combining Body-Fitted Grid Generation and Conjugate Gradient Methods for Shape Design in Heat Conduction Problems, *Numerical Heat Transfer, Part B*, Vol. 37, pp. 69-83, 2000.
18. Meric, A., Shape Optimization and Identification of Solid Geometries Considering Discontinuities, *Transactions of the ASME*, Vol. 110, pp. 544-550, 1988.
19. Meric, A., Differential and Integral Sensitivity Formulations and Shape Optimization by BEM, *Engineering Analysis with Boundary Elements*, Vol. 15, pp. 181-188, 1995.
20. Bialecki, R., Divo, E., Kassab, A.J. and Ait Maalem Lahcen, R., Explicit Calculation of Smoothed Sensitivity Coefficients for Linear Problems, *Int. J. Num. Methods in Eng.*, Vol. 57, No. 2, pp. 143-167, 2003.
21. Blackwell, B., Dowding, K., and Chochran, R.J., Development and Implementation of Sensitivity Coefficient Equations for Heat Conduction Problems, *Numerical Heat Transfer, Part B*, Vol. 36, pp. 15-32, 1999.
22. Brebbia, C.A., Telles, J.C.F. and Wrobel, L.C., *Boundary Element Techniques*, Springer-Verlag, Berlin, 1984.
23. Wrobel, L., C., *The Boundary Element Method - applications in thermo-fluids and acoustics*, Vol. 1, John Wiley and Sons, New York, 2002.
24. Divo, E. and Kassab, A.J., *Boundary Element Method for Heat Conduction with Applications in NonHomogeneous Media*, Wessex Institute of Technology Press, Boston, USA, 2003.
25. Divo, E., Kassab, A.J. and Rodriguez F., "An Efficient Singular Superposition Method for the Technique for Cavity Detection and Shape Optimization," *Inverse Problems in Engineering Mechanics IV: Proc. of ISIP 2003*, Masataka Tanaka, (Ed.), Elsevier Press, 2004.
26. Ulrich, T. W., Moslehy, F.A., and Kassab, A.J., A BEM Based Pattern Search Method for the Solution of the Inverse Elastostatics Problem, *Int. J. Solids and Structures*, Vol. 33, No. 15, pp. 2123-2131, 1996.
27. Kassab, A.J., Moslehy, F.A., and Daryapurkar, A., Nondestructive Detection of Cavities By An Inverse Elastostatics Method, *Engineering Analysis with Boundary Elements*, Vol. 13, No. 1, pp. 45-56, 1994.
28. Goldberg, D.E., *Genetic Algorithms in Search, Optimization and Machine Learning*, Addison-Wesley, Reading, MA, 1989.